CHAPTER IV

RESULTS AND DISCUSSION

1. Selection of medium for cell growth

The aim of this experiment was to select an appropriate medium composition for efficient propagation of Caco-2 cells. The required medium composition was the one that would result in small mean population doubling times (PDT) and/or be economical. In this study, three culture medium compositions were compared. Figure 10 displays growth curves of Caco-2 cells. Cell growth was in the lag phase for the first 2 days, after which it increased dramatically up to day 9 or 10 (log phase). The steady state (or plateau phase) was reached after 10 days. The PDT values derived from the growth curves and the cost of each medium are as shown in Table 4. In a preliminary report (Invitrogen, 2003), comparison between Dulbecco's Modified Eagle's Medium (DMEM) with 5% FBS supplement and Advanced DMEM with either 2% or 4% FBS supplement resulted in comparable cell growth in all three medium compositions. The authors suggested that use of Advanced DMEM was more economical and the amount of FBS supplemented could be reduced. However, the cell lines studied/used were not Caco-2 cells. Besides, DMEM used in that study was supplemented with only 5% FBS, whereas 10% FBS is usually recommended for Caco-2 (Lentz et al., 2000; Artursson, 1990; Liang, Chessic, and Yazdanian, 2000).

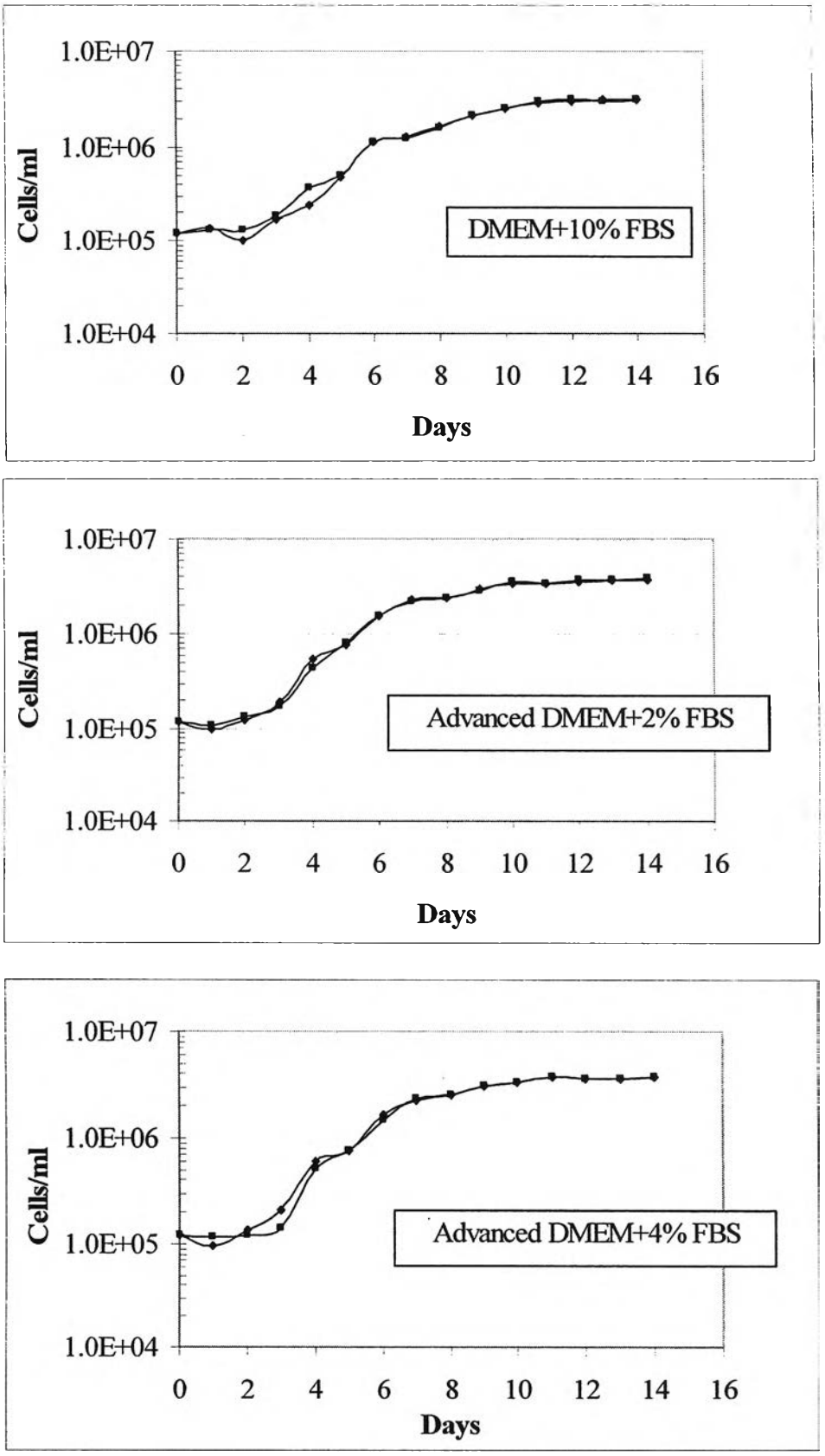

Figure 10: Growth curves of Caco-2 cells cultivated in three media (n=2)

Table 4: Population doubling times (PDT) and costs of DMEM with 10% FBS and Advanced DMEM with 2% and 4% FBS medium compositions. Data of PDT are shown as mean [actual values] of two separate experiments.

Medium composition	Population doubling time (hour)	Cost of medium (baht/liter)
DMEM + 10% FBS	32.34 [30.43, 34.50]	1500
Advanced DMEM + 2% FBS	27.58 [27.51, 27.65]	2300
Advanced DMEM + 4% FBS	27.25 [28.34, 26.16]	2500

From Table 4, PDT values of Advanced DMEM with 2% or 4% FBS were only slightly less than that of DMEM with 10% FBS. On the other hand, the overall cost of the medium using DMEM was lower, even though 10% FBS was used. Besides, most of research reports on Caco-2 cells used DMEM (Lentz et al., 2000; Artursson, 1990; Liang, Chessic, and Yazdanian, 2000), making the cell line well characterized with DMEM medium. In order to use Advanced DMEM, further characterization of cell morphology and function should be performed, which would be time and resource consuming. Thus, DMEM with 10% FBS was selected for Caco-2 cell culture in all experiments in this present study.

2. Characterization of Caco-2 monolayers

In order to use Caco-2 monolayers as a tool to study drug uptake and transport, the monolayers should be characterized in terms of integrity of the monolayer as well as functionality of the cells. The monolayers must (1) act as a sufficient barrier to hydrophilic substances, (2) be permeable to hydrophobic substances, and (3) express transport proteins of interest that function properly.

2.1 Integrity of Caco-2 monolayers as a barrier to hydrophilic substances

Cellular uptake of hydrophilic substances is usually difficult due to the lipophilic nature of cell membrane. Thus, transcellular transport is negligible for most hydrophilic

substances. Transport of these compounds across the monolayer can occur via the tight junction. This is known as the paracellular pathway. However, in order to use cell monolayers as a model to test whether a drug delivery system can increase uptake and/or transport of a hydrophilic compound via transcellular pathway, paracellular transport must be minimized. Caco-2 monolayers with good tight junction integrity should display transepithelial electrical resistance (TEER) of 300-1,400 $\Omega \cdot cm^2$ (Hidalgo, 2001; Borchard et al., 1996). Otherwise, the monolayer is considered leaky.

2.1.1 Transepithelial Electrical Resistance of Caco-2 monolayers

TEER measures the resistance to passive transport via tight junctions and reflects the confluence and tightness of monolayers. As seen in Figure 11, TEER values increased with culture time. At pre-confluence (day 7), however, the monolayer was leaky and TEER could not be measured. TEER values increased rapidly post-confluence. At day 21, the average TEER value was $1,319 \pm 63\ \Omega \cdot cm^2$. The results of this study are in good agreement with previous research where TEER values at 21 days were in the range of 300-1,400 $\Omega \cdot cm^2$ (Lentz et al., 2000; Liang, Chessic, and Yazdanian, 2000; Ward, Tippin, and Thakker, 2000; Artursson, 1990; Borchard et al., 1996). Results from different laboratories show a dramatic variability in TEER values. However, it is generally accepted that Caco-2 cell monolayers are suitable for transport study when TEER values exceed 300 $\Omega \cdot cm^2$ at 21 days after seeding (Walter and Kissel in 1995; Hunter, Hirst, and Simmons, 1993; Troutman and Thakker, 2003). Thus, these TEER values also show that Caco-2 monolayers used in this study could be classified as "tight" monolayers.

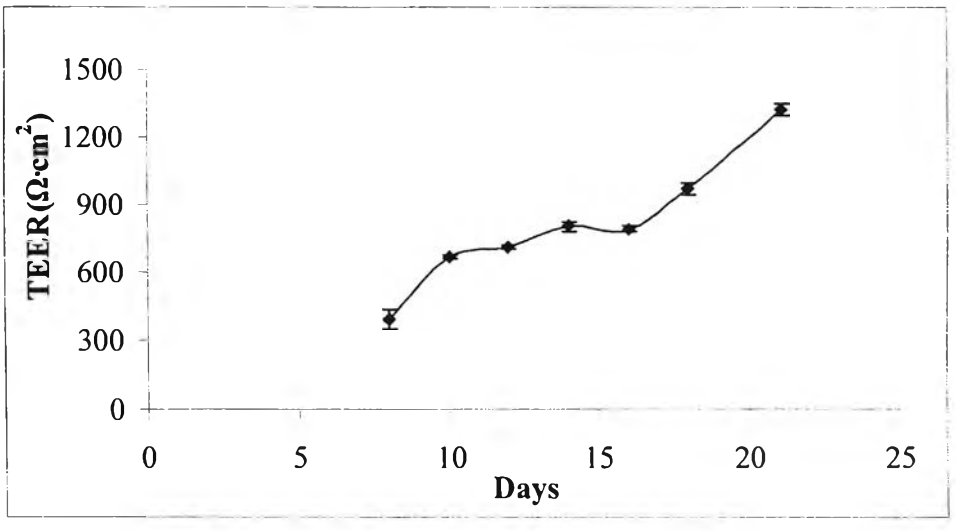

Figure 11: TEER values of Caco-2 monolayers as a function of time. Data are shown as mean ± SEM (n = 6).

2.1.2 Permeability of phenol red

Several hydrophilic markers have been used to validate Caco-2 monolayer integrity. These include some dyes such as Lucifer yellow (MW = 444.2) and phenol red (MW = 354.38). Tight monolayers are established when less than 1% of Lucifer yellow (Prueksaritanont et al., 1998) or 5% of phenol red (Martel, Monteiro, and Lemos, 2003) penetrates the monolayers per hour. In this study, phenol red was the hydrophilic marker employed to confirm integrity of Caco-2 monolayers. The concentration of phenol red in the basolateral compartment was less than 5 μM, which was the lower limit of quantification, at 1 hour. Accordingly, the calculated flux of phenol red through Caco-2 monolayers was less than 1.7% per hour. The basolateral buffer did not interfere with quantification of phenol red. This result confirms sufficient integrity of the Caco-2 monolayers used in the study.

2.2 Permeability of Theophylline

A model lipophilic compound with known passive transcellular transport, theophylline, was used to validate Caco-2 monolayers. The permeability should be

consistent and within the reported range in the literature. Theophylline has a molecular weight of 180.17 and is considered a highly permeable transcellular marker (apparent permeability > 1 x 10^{-6} cm/sec) (Artursson and Karlsson, 1991). Figure 12 shows the transport profiles of theophylline through Caco-2 monolayers. $P_{app, AB}$ values and $P_{app, BA}$ values for theophylline were significantly different ($p < 0.05$) (Table 5). The efflux ratio of Theophylline in the study was less than two (1.7). These results are consistent with theophylline being transported by passive diffusion.

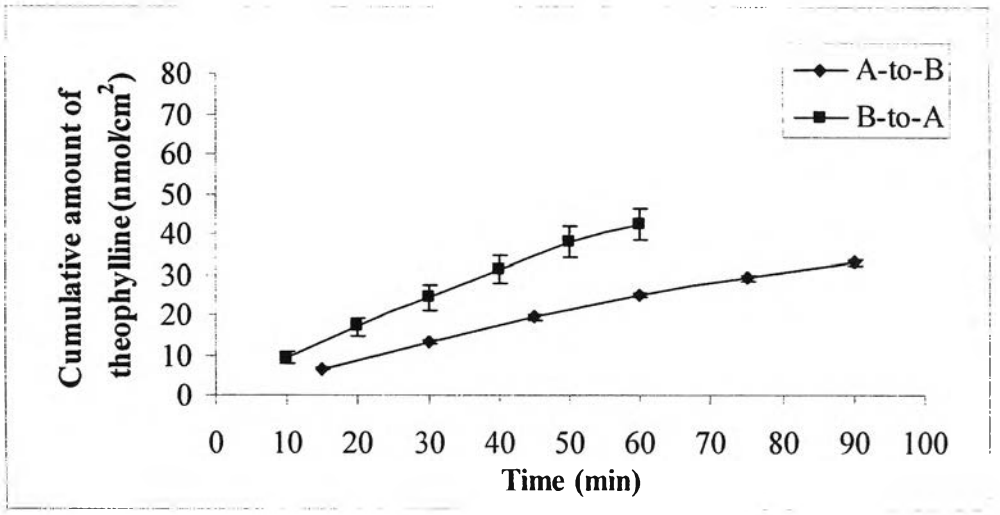

Figure 12: Absorptive (A-to-B, ♦) and secretory (B-to-A, ■) transepithelial transport profiles of theophylline across Caco-2 monolayers. Data are shown as mean ± SEM (n = 3).

Table 5: Apparent fluxes and permeability coefficients of theophylline transport across Caco-2 monolayers in the absorptive and secretory directions. Data are shown as mean ± SEM (n = 3).

Transport direction	Flux (nmol/cm²min)	Permeability coefficient (cm/s) x 10^5	TEER * (Ω·cm²)
Absorptive (A-to-B)	0.39 ± 0.02	3.24 ± 0.14	1,064/1,097
Secretory (B-to-A)	0.72 ± 0.06	5.58 ± 0.43	856/967

* TEER values of Caco-2 monolayers measured before/after the experiments

Permeability of theophylline across Caco-2 monolayers can vary between laboratories. Ingels and coworkers (2002) reported that $P_{app, AB}$ for theophylline across Caco-2 monolayer was 2.32 ± 0.03 x 10^{-5} cm/sec and $P_{app, BA}$ was 2.66 ± 0.06 x 10^{-5} cm/sec. Yamashita and coworkers (2000) reported that that $P_{app, AB}$ for theophylline across Caco-2 monolayer was 2.61 ± 1.5 x 10^{-5} cm/sec. On the contrary, Corti and coworkers (2006) reported higher $P_{app, AB}$ values of 4.65 ± 0.12 10^{-5} cm/sec for theophylline. The difference in the passage number of Caco-2 cells as well as other culturing conditions among laboratories is known to affect cell properties (Anderle et al., 1998; Freshney, 2000). This present study used Caco-2 cells in the passage number between 50 and 80, whereas Ingels and coworkers used those between 110 and 145. Yamashita and coworkers and Corti and coworkers used Caco-2 cells at passage number of 17 and 80-85, respectively. The $P_{app, AB}$ value of theophylline across Caco-2 monolayers in this experiment is within the range of the values previously reported. Therefore, Caco-2 monolayers cultivated under the conditions used in this study were a suitable model for evaluation of passive transcellular permeability.

2.3 Functional expression of P-glycoprotein efflux transporter

In order to show that Caco-2 monolayers could express P-glycoprotein (P-gp), absorptive and secretory apparent permeabilities of two substrates of P-gp were determined. The absorptive and secretory permeabilities of each compound were compared as the efflux ratio ($P_{app, BA}/P_{app, AB}$). The efflux ratio of more than 2 indicates that the drug is a substrate of efflux transporter(s) (Faassen et al., 2003).

2.3.1 Expression of efflux transporter

Caco-2 cells, which form an epithelium monolayer, are often used as a model for transport studies mediated by efflux transporters (Hunter, Hirst, and Simmons, 1993; Troutman and Thakker, 2003). In this study, Propranolol was selected as one of the two substrates to assess efflux transport characteristics of Caco-2 monolayers. Absorptive and secretory transepithelial profiles of propranolol are shown in Figure 13. These profiles indicate that the secretory flux is more than the absorptive flux. The calculated

fluxes, permeability coefficients, and efflux ratios are displayed in Table 6. The average $P_{app, BA}$ value for propranolol was significantly higher than the $P_{app, AB}$ value ($p < 0.05$). The efflux ratio of propranolol was 2.2 across the Caco-2 monolayers.

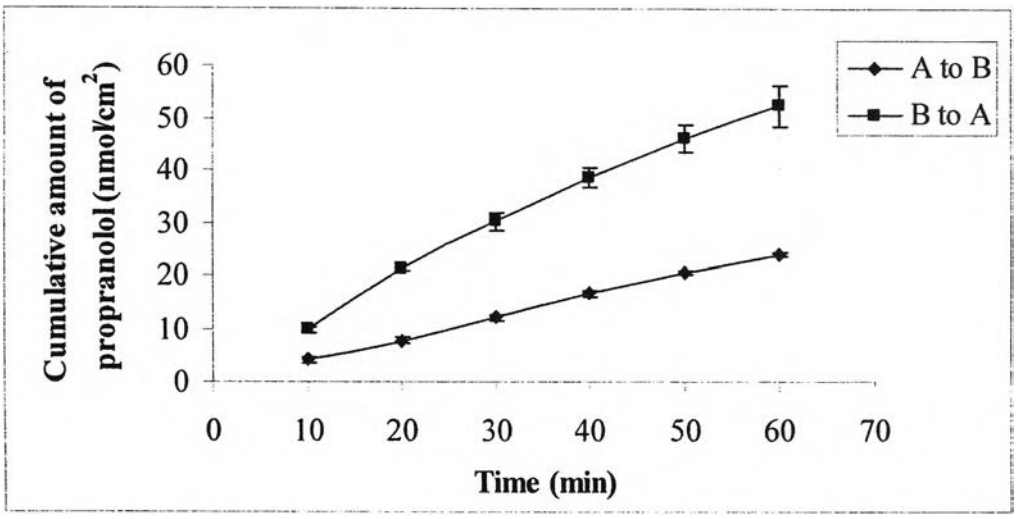

Figure 13: Absorptive (A-to-B, ♦) and secretory (B-to-A, ■) transepithelial transport profiles of propranolol across Caco-2 monolayers. Data are shown as mean ± SEM (n = 3).

Table 6: Apparent fluxes and permeability coefficients of propranolol transport across Caco-2 monolayers in the absorptive and secretory directions. Data are shown as mean ± SEM (n = 3).

Transport direction	Flux ($nmol/cm^2 min$)	Permeability coefficient ($cm/s) \times 10^5$	TEER ($\Omega \cdot cm^2$)
Absorptive (A-to-B)	0.41 ± 0.02	3.21 ± 0.08	1,235
Secretory (B-to-A)	0.85 ± 0.07	7.05 ± 0.53	1,251

Permeability as well as efflux ratio of propranolol also varies among laboratories. Vesantvoort and co-workers (2002) found that the efflux ratio of propranolol was dependent on the conditions of the experiment. When a pH gradient was present across the monolayer the efflux ratio was higher than in the absence of pH gradient (15.5 vesus 1.05). D'Emanuele and co-workers (2004) regarded propranolol as a P-gp substrate

with an efflux ratio of 2.6. The efflux ratio of propranolol in this study was more than two, which indicates expression of efflux transporter(s).

Another marker molecule that is known to display efflux transport is rhodamine 123. The cationic fluorescent dye was also used in this study. The absorptive and secretory profiles of rhodamine 123 are shown in Figure 14. The flux across fully confluent Caco-2 monolayers was linear with time up to 90 min. The average $P_{app, AB}$ for rhodamine 123 was 4.42 ± 0.28 x 10^{-7} cm/sec, which is significantly less than that observed in the opposite direction with the $P_{app, BA}$ of 28.1 ± 1.66 x 10^{-7} cm/sec (Table7). The efflux ratio of rhodamine 123 across Caco-2 monolayers was 6.36. This result also confirms that efflux proteins functionally existed. However, the resultant efflux ratio is considerably less than the values reported by Troutman and Thakker (2003) (efflux ratio = 11.4) and Suen, Simonian, and Threadgill (2004) (efflux ratio = 14.8). Many factors can influence expression of efflux transporters. These factors include culture time as well as culturing conditions such as passage number, composition of the medium, use of antibiotics, and subculturing protocol. Trypsinization of the cells after the culture has reached confluence leads to a decrease in P-gp expression levels, while trypsinization before confluence leads to an increasing expression of the protein after long-term cultivation (Anderle et al., 1998).

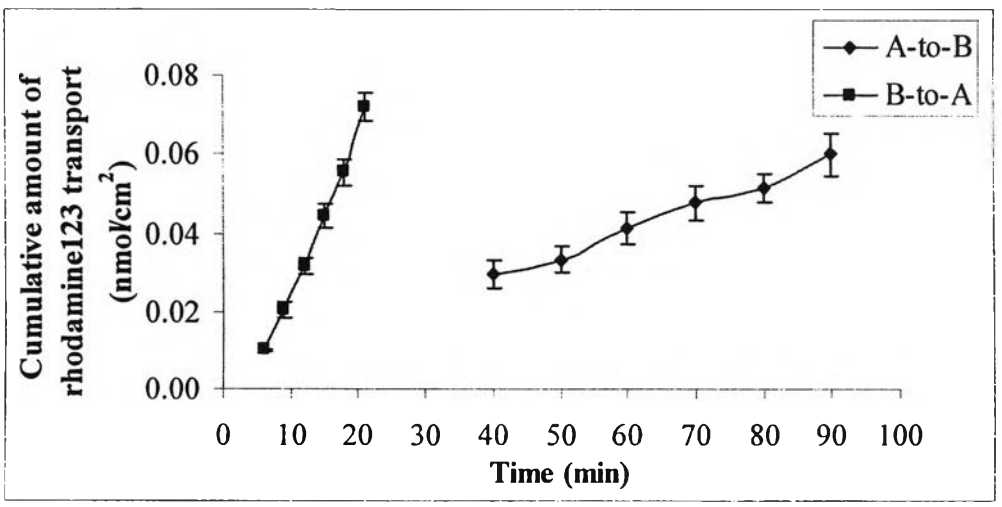

Figure 14: Absorptive (A-to-B, ♦) and secretory (B-to-A, ■) transepithelial transport profiles of rhodamine 123 across Caco-2 monolayers. Data are shown as mean ± SEM (n = 3).

Table 7: Apparent fluxes and permeability coefficients of rhodamine 123 transport across Caco-2 monolayers in the absorptive and secretory directions. Data are shown as mean ± SEM (n = 3).

Transport direction	Flux ($nmol/cm^2min$) x 10^4	Permeability coefficient (cm/s) x 10^7	TEER ($\Omega \cdot cm^2$)
Absorptive (A-to-B)	6.03 ± 0.44	4.42 ± 0.28	1,087
Secretory (B-to-A)	40.69 ± 2.39	28.10 ± 1.66	1,200

2.3.2 P-glycoprotein expression of Caco-2 monolayers

To determine whether P-gp mediated efflux transport was present on the apical side of Caco-2 cell monolayers, a potent specific inhibitor of P-glycoprotein, verapamil, was used. Verapamil is a competitive inhibitor of P-gp (Litman et al., 2001). Treatment of Caco-2 monolayers with this potent and selective P-gp inhibitor allowed measurement of rhodamine 123 (P-gp substrate) fluxes across Caco-2 cell monolayers without the influence of P-gp mediated efflux. Verapamil, at a concentration 100 μM, increased the transport of rhodamine 123 in the A-to-B direction (Figure 15). The average $P_{app,\ AB}$ value of rhodamine 123 was increased from 4.42 ± 0.28 x 10^{-7} cm/sec to 9.03 ± 0.76 x 10^{-7} cm/sec. On the contrary, a reduction in the B-to-A permeability was seen. The average $P_{app,\ BA}$ value of rhodamine 123 was reduced from 28.1 ± 1.66 x 10^{-7} cm/sec to 7.28 ± 0.45 x 10^{-7} cm/sec (Table 8). These differences were statistically significant ($p < 0.05$).

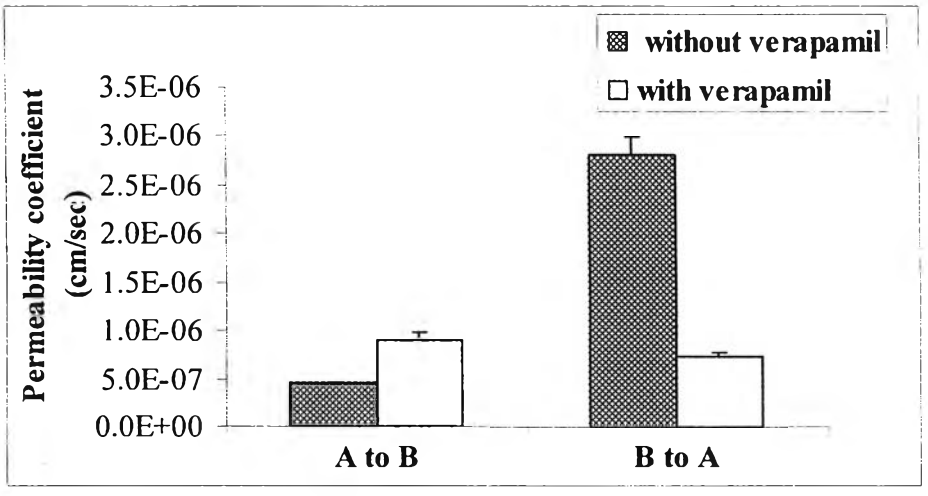

Figure 15: Absorptive and secretory permeability coefficients of rhodamine 123 across Caco-2 monolayers in the absence and in the presence of verapamil. Data are shown as mean ± SEM (n = 3).

Table 8: Apparent permeability coefficients of rhodamine 123 and the efflux activity of P-glycoprotein in absorptive and secretory directions across Caco-2 monolayers in the absence and in the presence of verapamil. Data are shown as mean ± SEM (n = 3).

Substrate (μM)	$P_{app, AB}$ x 10^7 (cm/s)	$P_{app, BA}$ x 10^7 (cm/s)	Efflux ratio
Rhodamine123 (20 μM)	4.42 ± 0.28	28.1 ± 1.66	6.36
Rhodamine123 (20 μM) +Verapamil (100 μM)	9.03 ± 0.76	7.28 ± 0.45	0.81

Inhibition of P-gp by verapamil produced an increase in the average $P_{app, AB}$ value of rhodamine 123 by 2.04 fold and decrease in the average $P_{app, BA}$ value of rhodamine 123 by 3.86 fold. The efflux ratio was reduced from 6.36 to 0.81. These results strongly indicate that the efflux system in Caco-2 cells involved P-gp. Similar approach to detect the expression of P-gp has been used by other groups (Hunter, Hirst, and Simmons, 1993; Troutman and Thakker, 2003; Korjamo et al., 2005).

Interestingly, in the presence verapamil (100 μM), the B-to-A transport profile of rhodamine 123 seemed to have two different slopes (Figure 16). The higher terminal slope started after 30 min. This result indicates that verapamil could efficiently inhibit P-gp transporter during the first 30 min, resulting in the small initial slope. After

30 min, when rhodamine 123 accumulated in the cells as the result of P-gp inhibition by verapamil, the dye could compete with verapimil in binding to P-gp. Thus, the dye was rapidly pumped out of the cells, resulting in the higher terminal slope. This phenomenon was not seen in the A-to-B direction.

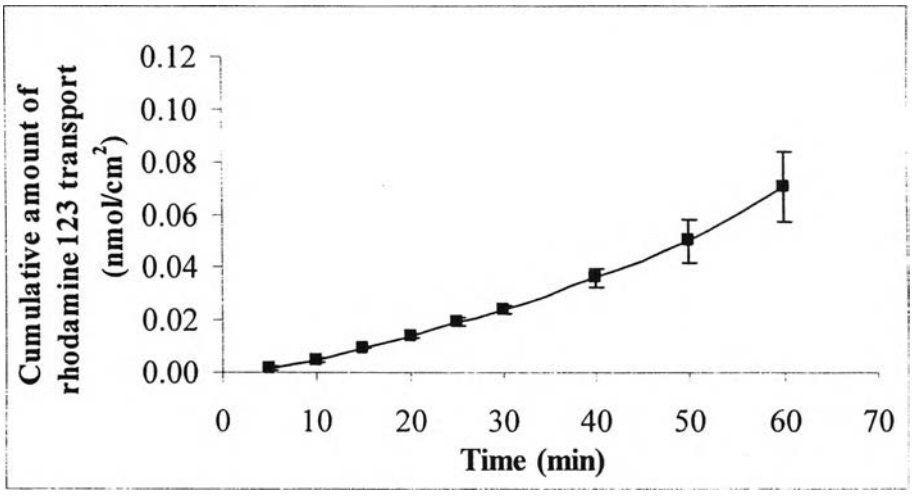

Figure 16: Secretory tranepithelial transport profile of rhodamine 123 in the presence of 100 μM verapamil. Data are shown as mean ± SEM (n = 3).

3. Effect of liposomes on accumulation of calcein in Caco-2 cells

3.1 Determination of calcein encapsulation efficiency

Non-encapsulated calcein was separated from calcein-loaded liposomes by gel filtration. Quantity of calcein encapsulated in liposomes was assayed using spectrofluorometric method. The mean entrapment efficiencies of calcein in neutral liposomes (PC/CH), positively charged liposomes (PC/SA/CH), and negatively charged liposome (PC/DCP/CH) were 5.95 ± 0.10%, 5.07%, and 6.89%, respectively. These values indicate that the entrapment efficiencies of calcein were rather similar among the three types of liposomes.

3.2 Effects of time after seeding and calcein concentration on accumulation of calcein in Caco-2 cells

Table 9 indicates that accumulation of calcein in Caco-2 cells was higher from liposomes than from solution in all cases ($p < 0.05$). Accumulation of calcein in Caco-2 cells was influenced by both the time after seeding and the concentration of calcein ($p < 0.05$). There was no interaction between time after seeding and calcein concentration ($p > 0.05$). Table 10 shows that the differences between the extents of uptake from liposomes and solution were most clearly seen when the time after seeding was 3 days. Thus, this time was selected for further experiments.

Table 9: Cell-associated calcein as a function of time after seeding and calcein concentration. Data are shown as mean ± SEM (n = 3).

Calcein concentration (μM)	Calcein uptake (μmol hr^{-1}) x 10^6					
	3 days		5 days		7 days	
	Solution	Liposomes	Solution	Liposomes	Solution	Liposomes
50	1.02 ± 0.24	8.27 ± 0.73	2.46 ± 0.57	7.72 ± 1.08	3.22 ± 0.08	9.54 ± 0.23
75	1.98 ± 0.24	9.78 ± 0.92	2.50 ± 0.58	9.64 ± 1.09	3.30 ± 0.30	11.6 ± 0.32
100	1.93 ± 0.23	9.11 ± 1.37	2.22 ± 1.00	9.33 ± 0.08	3.67 ± 0.56	12.9 ± 1.18

Table 10: Ratios of calcein uptake of calcein-loaded neutral liposomes to calcein solution

Calcein concentration (μM)	Ratio of calcein uptake (liposomes/solution)		
	3 days	5 days	7 days
0.050	8.07	3.15	2.96
0.075	4.95	3.86	3.50
0.100	4.73	4.21	3.52

3.3 Concentration dependence of calcein uptake by Caco-2 cells

Figure 17 shows the accumulation of calcein in Caco-2 cells from solution and from calcein-loaded liposomes at various calcein concentrations. The data indicate that the uptake of calcein from calcein solution and calcein-loaded liposomes depended on

calcein concentration. The liposomes gave higher calcein accumulation in the cells at all data points ($p < 0.05$). Calcein uptake as a function of calcein concentration was linear with solution, whereas the saturation profile was seen with liposomes. Calcein uptake started to plateau off at around 80 μM. Fluids are usually taken up by cells via pinocytosis and adsorption process can also take place (New, 1997). The data from calcein solution were consistent with these processes. On the other hand, calcein-loaded liposomes displayed the typical pattern of a saturable process. These data are consistent with a carrier-mediated process. The data agreed well with the hypothesis that liposomes were taken up into Caco-2 cells by endocytosis (Lodish et al., 2004). However, uptake of calcein-loaded liposomes may occur via fusion as well as via endocytosis, and adsorption process can also take place (New, 1997).

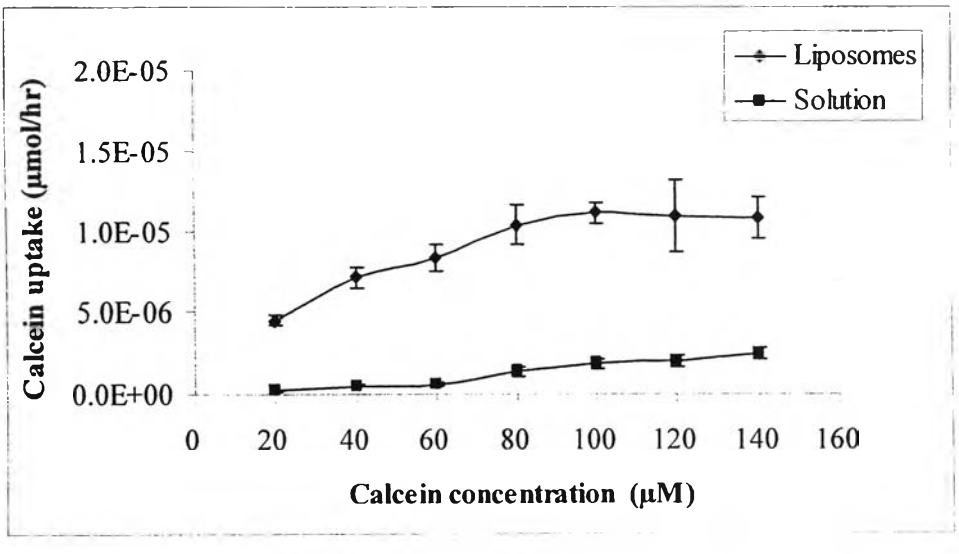

Figure 17: The intracellular accumulation of calcein from calcein solution and from calcein-loaded liposomes. Data are shown as mean ± SEM (n = 3).

3.4 Mechanism of cellular uptake of calcein-loaded liposomes

3.4.1 Effect of temperature on calcein uptake

Temperature affects fluid-phase endocytosis as well as endocytosis of small particles. Membrane lipids are in gel-like phase of low fluidity at temperature

below 27 °C, whereas temperature higher than 27 °C are required to obtain a liquid crystalline 'fluid' behaviour (Mamdouh et al., 1996). Fluidity of cell membrane affects activity of membrane bounded enzymes and transporter proteins (Rege, Kao, and Polli, 2002). All carrier-mediated processes are usually temperature sensitive, whereas adsorption is not. Thus, comparing the uptake rates at low and high temperatures can discriminate between these two processes (Schroeder and Kinden, 1983). The effect of temperature on calcein uptake from calcein solution and calcein-loaded liposomes is shown in Figure 18. The uptake of calcein from calcein-loaded neutral liposomes was significantly reduced at the lower temperature (4 °C). The calcein uptake was reduced from $5.35 \pm 0.19 \times 10^{-6}$ µmol/hr to $2.33 \pm 0.25 \times 10^{-6}$ µmol/hr. On the contrary, uptake of calcein from calcein solution was independent of temperature. The rates of calcein uptake from calcein solution at 37 °C and 4 °C were $5.00 \pm 0.92 \times 10^{-5}$ and $5.15 \pm 0.22 \times 10^{-5}$ µmol/hr, respectively.

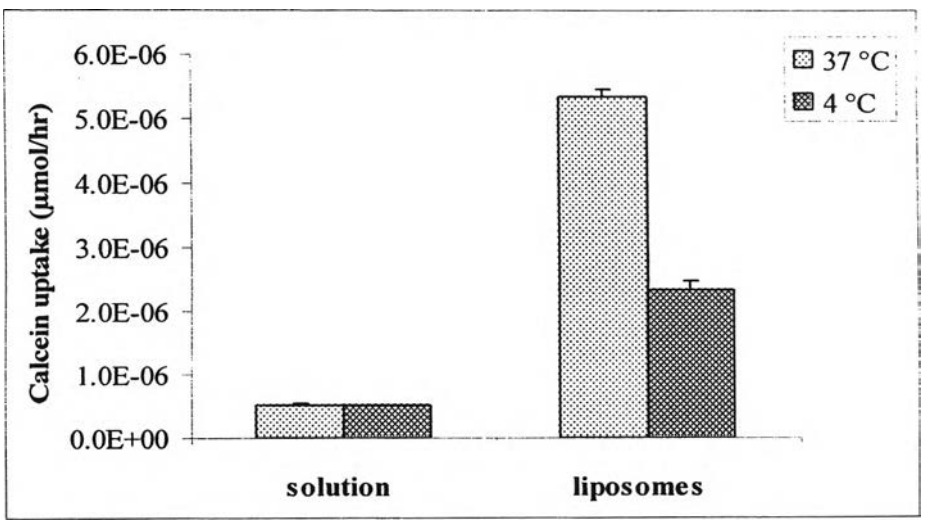

Figure 18: The intracellular accumulation of calcein in Caco-2 cells incubated with calcein solution and calcein-loaded liposomes (equivalent to 80 µM) at 37 °C and 4 °C. Data are shown as mean ± SEM (n = 3).

The results of this experiment were consistent with the hypothesis that liposomes were internalized into Caco-2 cells by an energy-dependent pathway, most probably by endocytosis. Lee and co-workers (1992) observed that kinetics of total association (uptake) of liposomes with cells was significantly faster at 37 °C than at 4 °C

in the murine macrophage-like cell line, J774. In general, the cellular uptake at 37 °C is a measure of the total association while the uptake at 4 °C is a measure of binding without any energy-dependent processes. Thus, calcein associated with Caco-2 cells from calcein solution seen in this study should be the result of binding rather than any internalization of the dye. This also agrees well with the previous results from calcein solution that cell-associated calcein increased slightly with calcein concentration without saturation.

3.4.2 Measurement of cell-associated calcein by flow cytometry

Flow cytometry is a laser technology that is used to measure characteristics of biological particles. Flow cytometry allows qualitative and quantitative examination of whole cells and cellular constituents that have been labeled with a wide range of available reagents such as dyes and monoclonal antibodies (Jaroszeski and Heller, 1998). The results of flow cytrometric study are displayed in Figure 19. Being self-quenched at high concentrations, calcein displays very little fluorescence until the solution is diluted with a consequent increase in fluorescence. Liposomes were loaded with high concentration of calcein (80μM) and would give little fluorescence if they were confined in the endosomes or lysosomes. The results show that cell-associated calcein (from both adsorption and intracellular accumulation) from solution was much stronger in fluorescence intensity than from calcein-loaded liposomes. The average fluorescence intensities associated with cells from calcein solution and calcein-loaded liposomes were 303.5 and 118.62, respectively.

A. Calcein solution

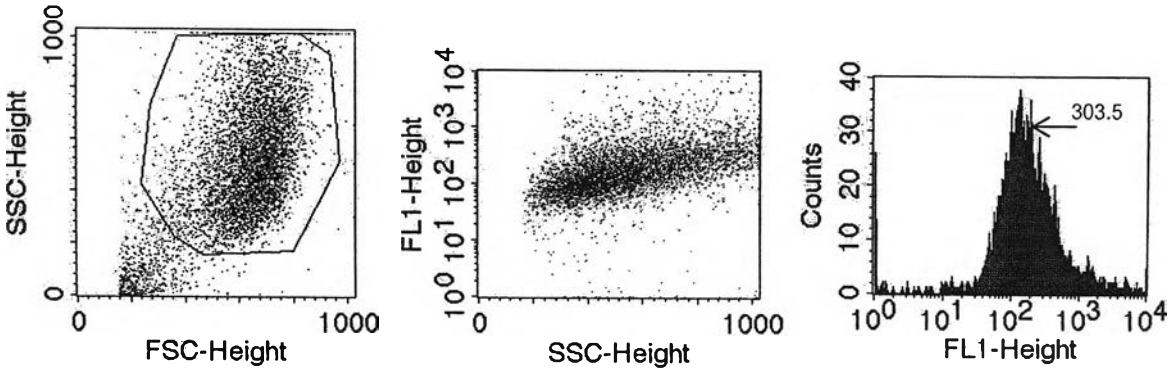

B. Calcein-loaded neutral liposomes

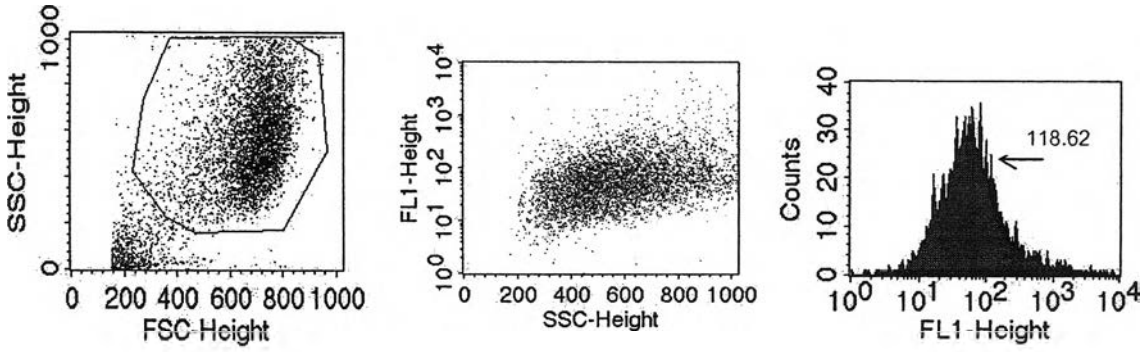

Sample	%Total	Mean	Geo Mean	CV	Median	Peak Ch
Solution	81.00	303.50	160.89	236.76	148.55	128
Liposomes	80.22	118.62	57.28	289.30	53.28	77

Figure 19: Cell-associated fluorescence intensities measured by flow cytometric method. (A) calcein solution and (B) calcein-loaded liposomes. FSC = forward angle light scatter, SSC = side-angle light scatter, and FL1 = fluorescent channel 1 for green fluorochrome, fluorescein isothiocyanate

On the other hand, when Caco-2 cells were digested with 1% Triton X-100, fluorescence intensity of calcein in cells was the opposite (Table 11). This result indicates that the total amount of calcein associated with cells was higher with calcein-loaded liposomes. The adsorption and intracellular accumulation of calcein from calcein-loaded neutral liposomes in Caco-2 cells was 10.7 fold of that seen with calcein solution. The overall results indicate that calcein-loaded liposomes were taken into

Caco-2 cells by endocytosis, not fusion. Liposomes are known to be endocytosed by other cells. Jansons and co-workers (1978) reported that neutral PC/CH (4:3) liposomes were taken up by L1210 cells via endocytosis rather than fusion. Endocytosis of liposomes were also reported by other research groups (Voinea and Simionescu, 2002; Fattal, Couvreur, and Dubernet, 2004).

Table 11: Total cell-associated calcein from calcein solution and calcein-loaded liposomes measured after cells were digested with 1% Triton X-100. Data are shown as mean ± SEM. (n = 3).

Sample	calcein concentration (μM)	Calcein uptake ($\mu mol\ hr^{-1}$) x 10^6
Solution	80	0.50 ± 0.09
Liposomes	80	5.35 ± 0.05

3.5 Effect of liposomal composition on calcein uptake by Caco-2 cells

The effect of surface charge on liposome uptake by Caco-2 cells was examined. The liposomes studied included PC/CH (7:3), PC/SA/CH or PC/DCP/CH (6:1:3). Calcein solution was used as a reference. The results indicate that interaction of liposomes with Caco-2 cells was also sensitive to liposome surface charge. Figure 20 shows that Caco-2 cells taken up calcein from all types of liposomes more efficiently than from calcein solution. Positively charged and neutral liposomes were taken up by Caco-2 cells more efficiently than negatively charged liposomes ($p < 0.05$) (~~Table 24~~). Because the surface of Caco-2 cells is also negatively charged, the calcein-loaded negatively charged liposomes could not bind well with the cells, making endocytosis less efficient. This result is consistent with a previous report that HeLa cells (human ovarian carcinoma cell) endocytoses positively charged liposomes (DOPC/DODAP 4:1, 20:1) better than negatively charged liposomes (DOPC/DOPS 4:1, 11:1) (Miller et al., 1998). In contrast, trophoblast cells take up neutral (PC/CH 1:1) and negatively charged liposomes (PC/CH/DCP 7:7:1) more avidly than positively chagred ones (PC/CH/SA 5:5:0.5) (Bajoria, Sooranna, and Contractor, 1997). In addition, CV1 cells (an African green monkey kidney cell line) more efficiently endocytose liposomes with negative surface

charge than those with neutral charge (PC/CHOL) (Lee et al., 1992). L929 (mouse murine fibroblast cells) and CL 18 (mouse myeloma) take up anionic liposomes (PS/CH 1:1) better than neutral liposomes (PC/CH 1:1) (Heath, Lopez, and Papahadjopoulos, 1985). Therefore, interaction of liposomes with cells depends on composition of lipid bilayer as well as cell type.

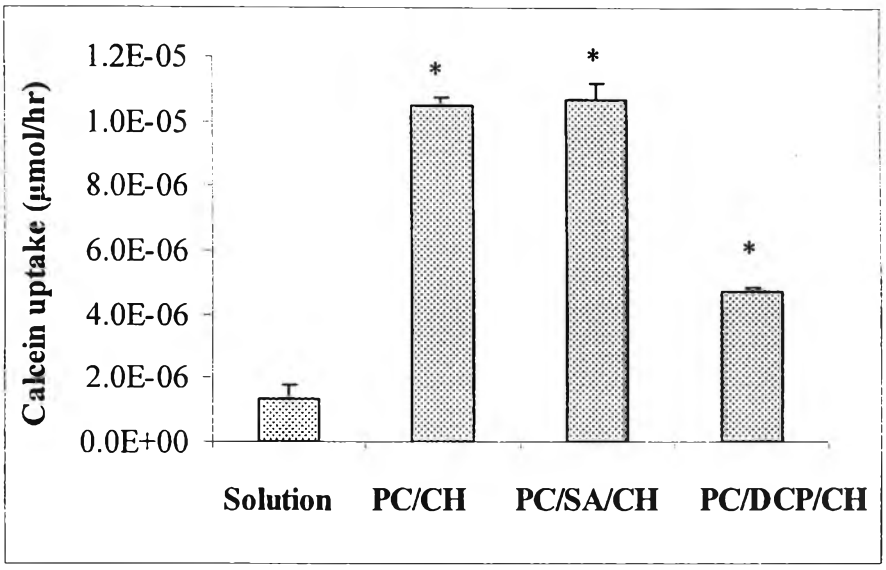

Figure 20: Cell-associated calcein from calcein solution, calcein-loaded neutral (PC/CH), cationic (PC/SA/CH), and anionic (PC/DCP/CH) liposomes. Data are shown as mean ± SEM (n = 3). * $p < 0.05$, compared with solution.

4. Effect of liposomes on transport of calcein across Caco-2 monolayers

Transcytosis is generally not an important process of uptake in epithelial cells of the GI tract. However, this process has been found in Caco-2 cells with approximately five times higher than that of normal human intestinal jejunum (Artursson, 1991). The aim of this part of study was to evaluate further, whether calcein taken into Caco-2 cells from liposomes via endocytosis would undergo exocytosis at any appreciable extents. Results are shown in Figure 21 and Tables 12-13. Transport was assessed by measurement of permeability coefficients of calcein-loaded neutral liposomes and calcein solution across Caco-2 monolayers. Figure 21 shows the transepithelial transport profiles

of calcein across Caco-2 monolayers in the absorptive direction. The flux of calcein from solution was more than 6-fold of the flux from the calcein-loaded neutral liposomes. As illustrated in Table 11, the apparent permeability coefficient (P_{app}) in the absorptive direction of calcein solution was also greater than that observed with calcein-loaded neutral liposomes. $P_{app,\ AB}$ values for calcein solution and calcein-loaded neutral liposomes were 7.67 ± 1.23 x 10^{-8} cm/sec and 1.18 ± 0.31 x 10^{-8} cm/sec, respectively. The flux of calcein from calcein solution was still less than 1% per hour, indicating that the monolayers were tight. However, the intracellular accumulation of fluorescence from calcein-loaded neutral liposomes was greater than that from calcein solution (Table 12). This result indicates that transcytosis did not occur with Caco-2 cells under the conditions used in this study. It appeared that when liposomes were taken up by Caco-2 cells, they were probably confined in endosomes and lysosomes. Calcein contents of in these structures could not penetrate the endosomal/lysosomal membrane into the cytoplasm as evident by flow cytometric study. Without transcytosis, calcein in endosomes and lysosomes was still self-quenched. Unquenching took place when the cells were digested with 1% Triton X-100, giving higher fluorescence intensity with liposomes than with solution. The overall results indicate that liposomes could increase the uptake of hydrophilic materials into Caco-2 cells, but transcytosis did not occur efficiently enough to be of any use in enhancing transport of hydrophilic substances across the cells.

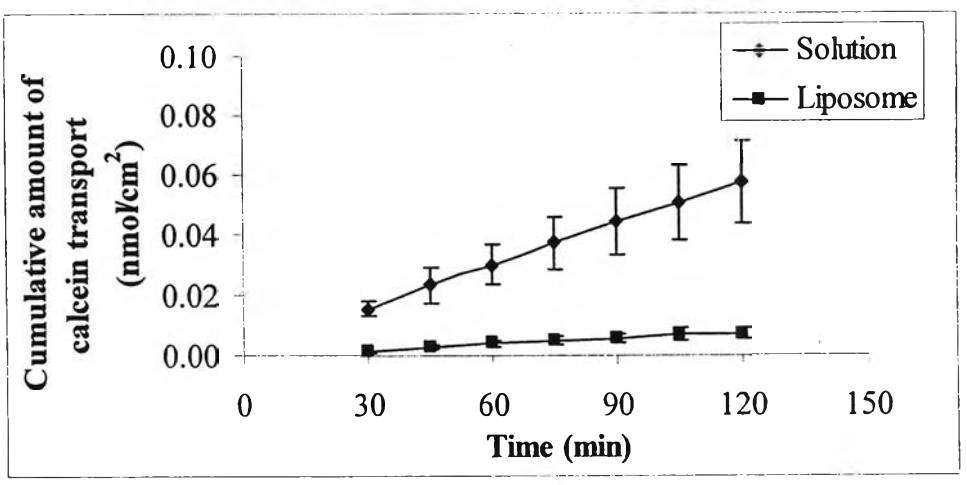

Figure 21: Absorptive transepithelial transport profiles of calcein from calcein solution and calcein-loaded neutral liposomes across Caco-2 monolayers. Data are shown as mean ± SEM (n = 3).

Table 12: Apparent fluxes and permeability coefficients of calcein in the absorptive direction from calcein solution and calcein-loaded neutral liposomes across Caco-2 monolayers. Data are shown as mean ± SEM (n = 3).

Treatment	Flux ($nmol/cm^2min$) x 10^3	permeability coefficient (cm/sec) x 10^8	TEER* ($\Omega \cdot cm^2$)
Solution	0.42 ± 0.07	7.67 ± 1.23	1,290/1,390
Neutral liposomes	0.07 ± 0.02	1.18 ± 0.31	1,349/1,380

* TEER values of Caco-2 monolayers measured before/after the experiments

Table 13: Accumulation of calcein from calcein solution and calcein-loaded neutral liposomes in Caco-2 cells during transport study. Data are shown as mean ± SEM (n = 3).

Treatment	Calcein accumulation in cells (ng)			Mean ± SEM
	1	2	3	
Solution	148.03	136.39	137.51	140.64 ± 3.71
Neutral liposomes	204.37	248.44	259.89	237.57 ± 16.92

5. Effect of liposomes on efflux of rhodamine 123

5.1 Effect of liposomes and phospholipids on accumulation of rhodamine 123 in Caco-2 cells

When Caco-2 monolayers were pre-incubated with and without blank liposomes, no significant effect on rhodamine 123 uptake was seen ($p > 0.05$) (Figure 22). This indicates that soybean PC used in this study did not show any competition with rhodamine 123 in binding with P-gp on the apical membrane of Caco-2 cells. This result is in contrast with a previous study with epirubicin, another P-gp substrate. Dipalmitoyl phosphatidylcholine and dipalmitoyl phosphatidylethanolamine compete with epirubicin in binding with P-gp and increase secretion of the drug (Lo, 2000). The discrepancy seen here might be attributed to the differences in the type of phospholipids as well as the binding kinetics and the binding affinity of the two substances (rhodamine 123 versus epirubicin). The lipids used in the previous study were in gel state, but soybean PC was in liquid crystalline state at the temperature used. Fluidity of liposomal membranes often

plays important roles in their interactions with cells (Mamdouh et al., 1996). However, with rhodamine 123-loaded liposomes, the dye accumulated in Caco-2 cells 3.16 times of that seen with rhodamine 123 solution. This result indicates that liposomes could significantly increase uptake of rhodamine 123, most likely by bypassing the activity of P-gp (Lo, 2000).

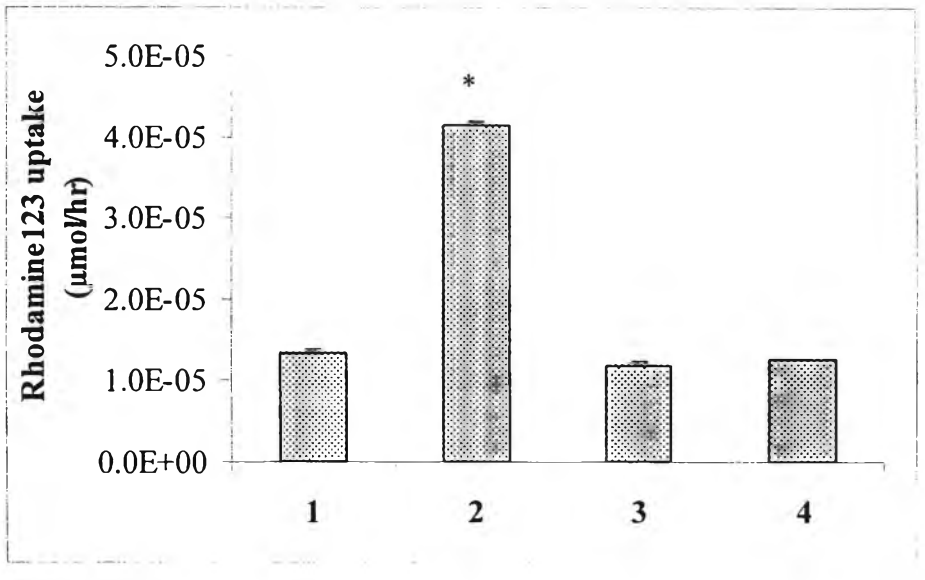

Figure 22: Cell-associacted rhodamine 123 from different formulations: (1) rhodamine 123 solution, (2) rhodamine 123-loaded liposomes, (3) blank liposomes + rhodamine 123 solution and (4) blank liposomes + rhodamine 123 solution, pretreated with blank liposomes. Data are shown as mean ± SEM (n = 3). * $p < 0.05$, compared with solution.

5.2 Effect of verapamil on the uptake of rhodamine 123 from liposomes by Caco-2 cells

Whenever Caco-2 cells were pre-incubated with 100 µM verapamil for 30 min, uptake of rhodamine 123 significantly increased from both rhodamine 123 solution and rhodamine 123-loaded liposome ($p < 0.05$). This effect was not seen when rhodamine 123 solution was co-incubated with blank liposomes ($p > 0.05$). The reverse ratio is highest in the case of rhodamine 123 solution. This result indicates that rhodamine 123 from solution was easily pumped out by P-gp than from liposomes. Besides, liposomes were likely to increase internalization of rhodamine 123 by Caco-2 cells since the uptake

from liposomes was higher than that from solution in the presence of verapamil. On the contrary, blank liposomes might interfere with the interaction between verapamil and P-gp since the effect of verapamil was less than expected in the presence of blank liposomes.

Table 14: Cell-associated rhodamine 123 from rhodamine 123 solution, rhodamine 123-loaded liposomes, and blank liposomes with rhodamine 123 solution in the presence and in the absence of 100 μM verapamil. Data are shown as mean ± SEM (n = 3).

Treatment	Uptake of rhodamine 123 (μmol hr^{-1}) x 10^5		Reverse ratio	P-value
	without verapamil	with verapamil		
Solution	1.31 ± 0.05	3.10 ± 0.21	2.366	0.008
Liposomes	4.14 ± 0.06	5.93 ± 0.10	1.432	0.001
Solution with blank liposomes	1.18 ± 0.05	1.43 ± 0.03	1.212	0.051

5.3 Measurement of cell-associated rhodamine 123 by flow cytometry

Figure 23 shows that the cell-associated fluorescence intensity from rhodamine123-loaded neutral liposomes was much stronger than that from rhoamine123 solution with average values of 653.13 and 304.90, respectively. The results are consistent with the hypothesis that endocytosis was the mechanism of uptake of liposomes by Caco-2 cells. During process of breakdown of liposomes in endosomes or lysosomes, rhodamine 123 was released. Since rhodamine 123 is lipophilic, it could penetrate endosomal/lysosomal membranes into the cytoplasm. Dilution of rhodamine 123 in the cytoplasm resulted in unquenching of the dye. This finding is opposite to what was seen with calcein, which is a water-soluble fluorescent dye.

A. Rhodamine 123 solution

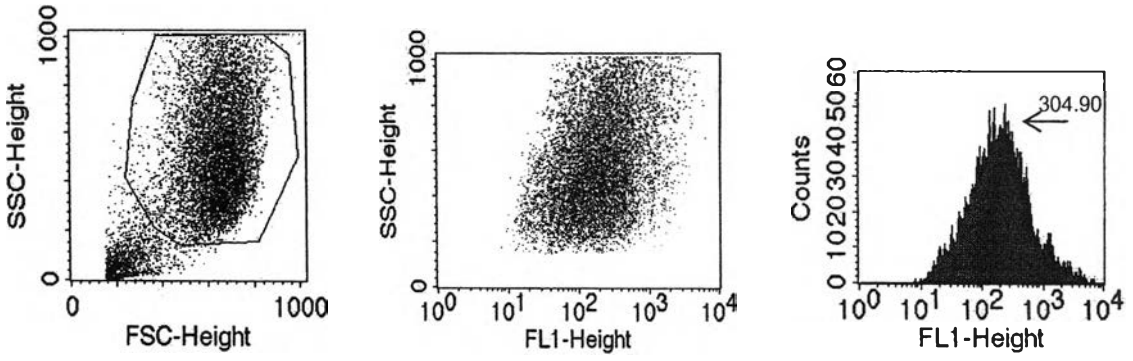

B. Rhodamine 123-loaded neutral liposomes

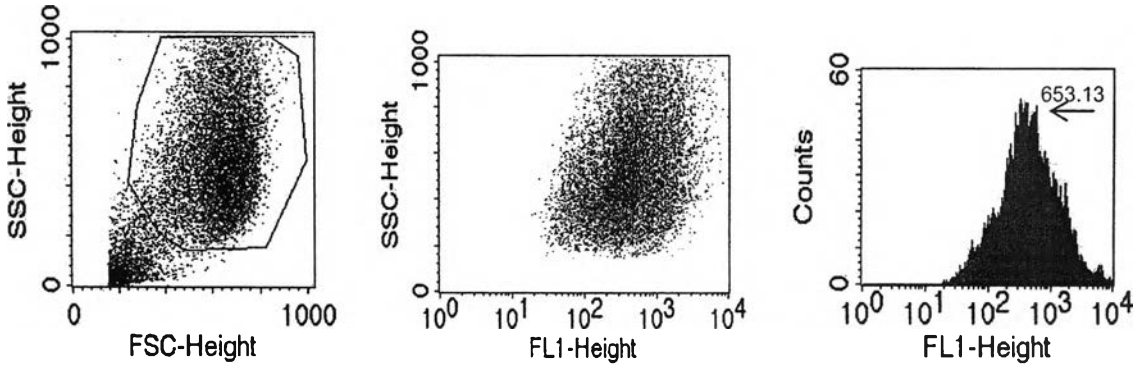

Sample	%Total	Mean	Geo Mean	CV	Median	Peak Ch
Solution	77.29	304.90	177.05	140.44	176.24	224
Liposomes	73.77	653.13	404.35	120.92	399.54	302

Figure 23: Results of flow cytometric study of Caco-2 cells incubated with (A) rhodamine 123 solution and (B) rhodamine 123-loaded neutral liposomes. FSC = forward angle light scatter, SSC = side-angle light scatter and FL1 = fluorescent channel green fluorochrome fluorescein isothiocyanate

5.4 Effect of liposomal composition on the uptake of rhodamine 123

Physical appearances of the three types of liposomes are shown in Figure 24. Rhodamine 123-loaded negatively charged and positively charged liposomes were more translucent than rhodamine 123-loaded neutral liposomes. This result implies that the former two types of liposomes might have smaller sizes than the latter. Size and size

distribution could not be determined in this study since the presence of rhodamine 123 would interfere with the photon correlation spectroscopy, the technique that is proper for small liposomes (New, 1997). Figure 25 and Table 15 show that the uptake of rhodamine 123-loaded neutral liposomes was significantly higher than those of the other two types of liposomes and the solution ($p < 0.05$). Rhodamine 123 uptake from the latter two types of liposomes, on the contrary, was significantly lower than that from the solution ($p < 0.05$). These results agree well with the previous finding that the most appropriate size of liposomes for endocytosis is 100-200 nm (Heath, Lopez, and Papahadjopoulos, 1985).

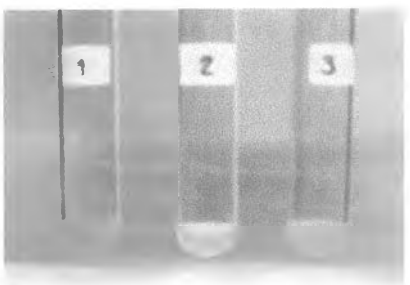

Figure 24: Physical appearances of (1) rhodamine 123-loaded neutral liposomes, (2) rhodamine 123-loaded positively charged liposomes, and (3) rhodamine 123-loaded negatively charged liposomes.

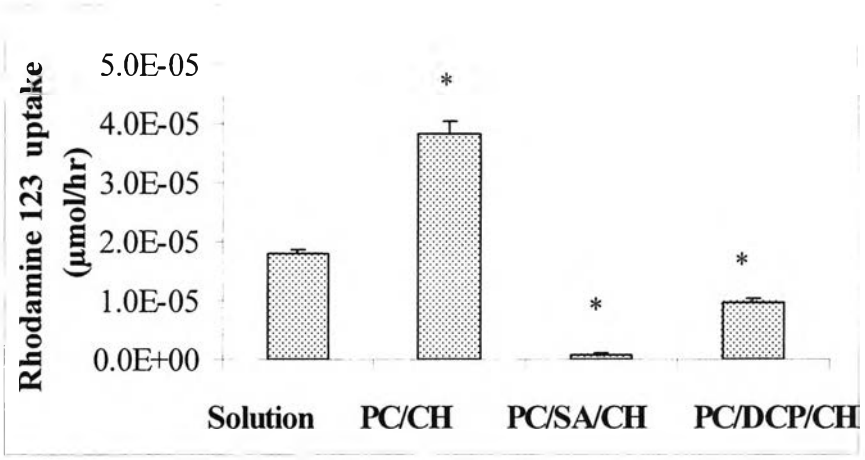

Figure 25: Cell-associated rhodamine 123 from rhodamine 123 solution, rhodamine 123-loaded neutral (PC/CH), positively charged (PC/SA/CH) and negatively charged (PC/DCP/CH) liposomes. Data are shown as mean ± SEM ($n = 3$). * $p < 0.05$, compared with solution.

Table 15: Cell-associated rhodamine 123 from rhodamine 123 solution, rhodamine 123-loaded neutral (PC/CH), positively charged (PC/SA/CH) and negatively charged (PC/DCP/CH) liposomes. Data are shown as mean ± SEM (n = 3).

Treatment	Uptake of rhodamine 123 (mmol hr^{-1}) x 10^5
Solution	1.79 ± 0.09
Neutral liposomes	3.83 ± 0.19
Positively charged liposomes	0.09 ± 0.03
Negatively charged liposomes	0.97 ± 0.59

6. Effect of liposomes on transport of rhodamine 123 across Caco-2 monolayers

In this experiment, only neutral liposomes were used since they gave the highest accumulation of rhodamine 123 in Caco-2 cells. Transport was assessed with measurement of permeability coefficient of rhodamine 123-loaded neutral liposomes and rhodamine 123 solution across Caco-2 monolayer. The transport profiles of rhodamine 123 from solution and from rhodamine 123-loaded liposomes are displayed in Figure 26. Table 16 shows that the flux and the apparent permeability coefficient of rhodamine 123 from rhodamine 123-loaded neutral liposomes were significantly higher than those obtained from rhodamine 123 solution ($p < 0.05$). This result indicates that neutral liposomes could facilitate transport of rhodamine 123 across Caco-2 monolayers. Though transcytosis did not occur to an appreciable extent in Caco-2 cells, rhodamine 123 could penetrate the cellular membrane of the cells since the dye is lipophilic. This result agrees with the previous report with epirubicin where transport of the liposome-associated drug is higher than that of epirubicin solution (Lo, 2000). The overall results indicate that liposomes should be useful in increasing uptake of P-gp substrates and in facilitating transport of such molecules across Caco-2 monolayers.

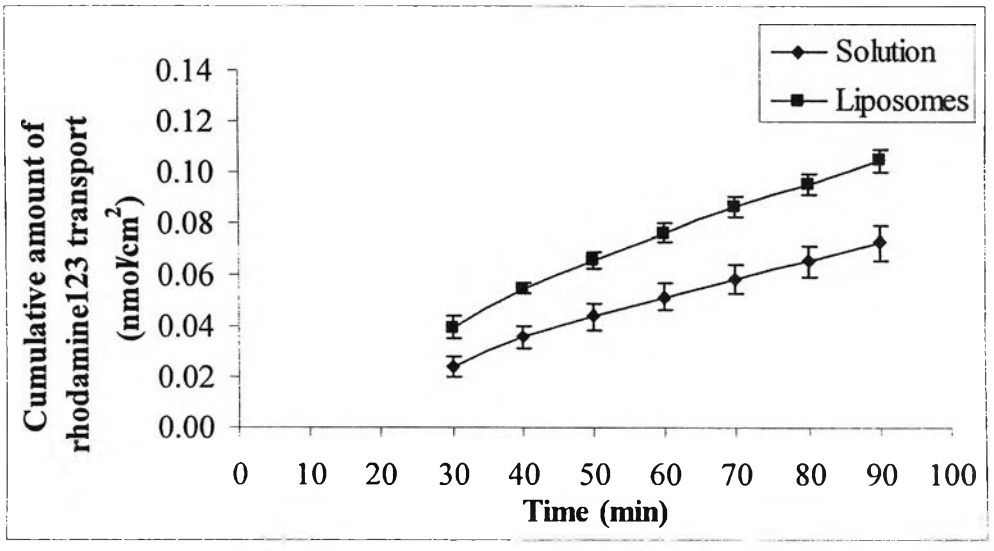

Figure 26: Tranepithelial transport profiles of rhodamine 123 from solution and rhodamine 123-loaded neutral liposomes across Caco-2 monolayers. Data are shown as mean ± SEM (n = 3).

Table 16: Apparent fluxes and permeability coefficients in the absorptive direction of rhodamine 123 from rhodamine 123 solution and rhodamine 123-loaded neutral liposomes across Caco-2 monolayers. Data are shown as mean ± SEM (n = 3).

Treatment	Flux ($nmol/cm^2 min$) x 10^4	Permeability coefficient (cm/s) x 10^7	TEER * ($\Omega \cdot cm^2$)
Solution	7.78 ± 0.43	7.05 ± 0.39	1,223/1,006
Neutral liposomes	10.6 ± 0.21	9.62 ± 0.19	1,284/1,151

* TEER values of Caco-2 monolayers measured before/after the experiments